

# Selective synthesis of alkyl poly- $\beta$ -D-glucopyranoside over mixed metal oxide

Nivedita S. Chaubal, Vishal Y. Joshi, Manohar R. Sawant\*

Department of Chemistry, Institute of Chemical Technology (Autonomous), University of Mumbai, Matunga, Mumbai 400 019, India

Received 20 September 2006; accepted 14 November 2006  
Available online 19 November 2006

## Abstract

Glycosylation reactions are most commonly encountered in nature. Synthetically, glycosylation is carried out with Lewis acid catalyst, HF,  $\text{AlCl}_3$  or mineral acids. However environmental threat associated with such catalysts has encouraged process modification and the development of solid catalyzed glycosylation reactions, which are commercially viable as well. In this contribution comparative study of glycosidic bond formation of simple D-glucose with several fatty alcohols ( $\text{C}_8$ – $\text{C}_{14}$ ) over variety of mixed metal oxidic spinels ( $\text{CuFe}_2\text{O}_4$ ,  $\text{ZnFe}_2\text{O}_4$ ,  $\text{CoFe}_2\text{O}_4$  and  $\text{NiFe}_2\text{O}_4$ , 10% (w/w)  $\text{ZnFe}_2\text{O}_4$  supported on  $\text{SiO}_2$  and  $\text{ZrO}_2$ ) is taken up to evaluate the performance of this potential catalysts system. Effect of catalyst preparation was evaluated. This replacement of homogeneous acid catalyst by oxidic spinels shows alkyl poly  $\beta$ -D-glucopyranoside as major product at comparatively low temperature range. The effects of variety of parameters were studied in a batch reactor. The mechanism of the reaction over mixed metal oxidic spinels at 363 K is put forth.

© 2006 Elsevier B.V. All rights reserved.

**Keywords:** Alkyl poly- $\beta$ -D-glucopyranoside; Poly-glucose; Spinel; Glycosidic bond formation

## 1. Introduction

Alkyl poly- $\beta$ -D-glucopyranoside act as a novel class of surfactants, which are useful as food bulking agents, reduced calorie sweeteners, fat replacement agents for food products, stabilizing agents for food and beverage products, thickening and emulsifying agents for food products, adhesives, biodegradable plastic and films, sizing agents for paper and textile, ethical pharmaceuticals and new fibers. The development of stereo selective methods for the synthesis of glycosidic linkages presents a considerable challenge to synthetic chemists [1–3]. Although well developed chemical synthesis of glycoside involves selective protection, deprotection and coupling using a metal catalyst. Glycosylation of simple alcohols with D-glucose can be performed by strong acids like  $\text{BF}_3$ -etherate [4], HCl [5], *para* toluene sulphonic acid and  $\text{H}_2\text{SO}_4$  [6] to give both  $\alpha$ - and  $\beta$ -anomer with high degree of polymerization of glucose unit. Such glycosylation are normally carried

out, in only moderate yield (40–50%). This problem in synthesis has promoted the development of cost effective and less toxic promoter based synthetic route. Toshima and coworkers [7] used montmorillonite K-10 as a heterogeneous solid catalyst for glycosidation of olivoses. Later on, same research group used montmorillonite K-10 with benzyl-protected glucopyranosyl phosphate and several alcohols to get  $\beta$ -O-glycosidic linkages in more than 80% Yield [8]. In previous studies [9], we have demonstrated stereoselective  $\beta$ -D-glucopyranosylation of 2,3,4,6-tetra-*o*-acetyl- $\alpha$ -D-glucosyl bromide and fatty alcohols over  $\text{LiCO}_3$  as reaction promoter. Such reaction promoter has limited activity and catalytic life. Highly effective and recyclable glycosidation methods without halogenations have attracted our attention. Hence in this work, the glycosylation of D-glucose with several fatty alcohols in liquid phase has been investigated on a series of mixed metal oxides catalyst prepared by co-precipitation method, crystallizing with spinel lattice such as,  $\text{CuFe}_2\text{O}_4$ ,  $\text{ZnFe}_2\text{O}_4$ ,  $\text{CoFe}_2\text{O}_4$ ,  $\text{NiFe}_2\text{O}_4$  and 10% (w/w)  $\text{ZnFe}_2\text{O}_4$  supported on  $\text{SiO}_2$  and  $\text{ZrO}_2$ . The choice of catalyst as a spinel system is due to two reasons; first, spinel lattice imparts extra stability to the catalysts under various reaction conditions. Secondly, mixed metal oxides do not lose their catalytic activ-

\* Corresponding author. Tel.: +91 22 2414 5616; fax: +91 22 2414 5614.  
E-mail address: [mrsawant2@rediffmail.com](mailto:mrsawant2@rediffmail.com) (M.R. Sawant).

ity due to aging and formation of carbon over the surface so these systems have sustained activity for longer duration [10]. The best catalyst for the selective preparation of alkyl poly- $\beta$ -D-glucopyranoside was 10% (w/w)  $\text{ZnFe}_2\text{O}_4$  supported on  $\text{ZrO}_2$ . A 10% (w/w)  $\text{ZnFe}_2\text{O}_4/\text{ZrO}_2$  prepared by co-precipitation method was compared with 10% (w/w)  $\text{ZnFe}_2\text{O}_4/\text{ZrO}_2$  prepared by template route for the selective formation alkyl poly- $\beta$ -D-glucopyranoside. The major product was alkyl poly- $\beta$ -D-glucopyranoside with some poly glucose formation as a side product.

## 2. Experimental

### 2.1. Materials and chemicals

Nitrates of zinc, copper, iron and zirconium oxychloride of analytical reagent were used for catalyst preparation. A 30%  $\text{H}_2\text{O}_2$ ,  $\text{SiO}_2$  of mesh size 200 were used; D-glucose and fatty alcohols (in range from  $\text{C}_8$  to  $\text{C}_{14}$ ) of analytical grade were used with out further purification. The catalyst was prepared using co-precipitation technique and template route.

### 2.2. Synthesis of catalysts

#### 2.2.1. Co-precipitation technique [10–12]

To prepare the catalyst an aqueous solution containing the desired ions in the required molar proportions was prepared by dissolving the salts in the stoichiometric proportion in distilled water. It was precipitated by sodium hydroxide and the pH of the solution was maintained 9–9.5. The precipitate was digested at 353 K in water bath for 3 h and then oxidized by drop wise addition of required amount of 30%  $\text{H}_2\text{O}_2$  with constant stirring for obtaining single phase spinel. After completion of reaction the resultant precipitate was dried at 383 K for 3 h then calcined at 1173 K for 9 h. Similarly  $\text{ZrO}_2$  was prepared by co-precipitation procedure from  $\text{ZrOCl}_2 \cdot 7\text{H}_2\text{O}$ .  $\text{SiO}_2$  of mesh size 200 was taken as available in the market.

A 10%  $\text{ZnFe}_2\text{O}_4$  catalyst supported on  $\text{SiO}_2$  and  $\text{ZrO}_2$  was prepared by incipient wetness method by impregnating the aqueous solution of nitrates of required ion in a stoichiometric amount on the support; they were dried at 393 K for removal of water and other volatile material and subsequently calcined at 1173 K for 9 h.

#### 2.2.2. Templated approach [13]

In a typical preparation, Fe and Zn nitrates were taken in, stoichiometric amounts (2:1) and were dissolved in 10 ml of methanol to this 10 ml of decyl polyglycoside (50%) aqueous solution was added with vigorous stirring for 1 h. The resulting solution was gelled at 303 K for 20 h (catalyst preparation is optimized). Similarly  $\text{ZrOCl}_2 \cdot 7\text{H}_2\text{O}$  was treated with decyl polyglycoside (50%) aqueous solution and gelled at 303 K for 20 h. Both, Fe + Zn and Zr gel were mixed together aged for 5 h, dried at 373 K. This as made bulk sample was calcined at 1173 K for 9 h in air to remove the surfactant to obtain 10% (w/w) of  $\text{ZnFe}_2\text{O}_4$  on  $\text{ZrO}_2$ .

### 2.3. Characterization of 10% (w/w) of $\text{ZnFe}_2\text{O}_4$ on $\text{ZrO}_2$ prepared by co-precipitation and templated approach

Catalysts were characterized by X-ray diffraction, BET surface area measurement, FT-IR and SEM.

### 2.4. Reaction methodology and product analysis

The reactor consisted of a standard flat bottom cylindrical vessel of 5 cm, i.e. of 100 ml capacity equipped with four equi-spaced baffles, a pitched-bladed turbine impeller and a condenser. The assembly was kept in an isothermal oil bath at a known temperature and mechanically agitated with an electric motor. Melting points were determined using capillary method. Specific rotations were recorded on a manual polarimeter. Infrared spectroscopy was recorded on Model 500 Spectrophotometer, Buck Scientific Inc.  $^1\text{H NMR}$  were recorded on model of Hitachi Inc. and operated at 300 MHz. All the data are uncorrected. Each catalyst was studied for its catalytic behavior towards glycosidic bond formation with several fatty alcohols at the 363 K. In a typical reaction D-glucose (10 mmol) in toluene (16 ml) was stirred for 15 min at room temperature. Then catalysts and fatty alcohols ( $\text{C}_{8-14}$ , 20 mmol) was added, the reaction carried at 363 K for stipulated time depending upon the nature of substrate. Reaction mass was cooled and filtered over celite. Filtrate was evaporated in vacuum and the resulting material was purified by column chromatography (toluene/ethyl acetate = 15/5) to afford alkyl poly  $\beta$ -D-glucopyranoside.

## 3. Results and discussion

### 3.1. Catalyst characterization

#### 3.1.1. XRD of catalysts samples prepared by co-precipitation method

As shown in Fig. 1 XRD of  $\text{ZnFe}_2\text{O}_4$  (a) showed crystalline single-phase spinel structure with  $d$  (Scherrer equation) =  $10 \text{ \AA}$ ,  $a = 8.398 \text{ \AA}$  which is comparable to the authentic  $\text{ZnFe}_2\text{O}_4$  in JCPDS file. XRD of  $\text{ZrO}_2$  (b) shows intense peaks indicating crystalline nature of  $\text{ZrO}_2$ . XRD of  $\text{ZnFe}_2\text{O}_4/\text{ZrO}_2$  (c) shows the formation of  $\text{ZnFe}_2\text{O}_4$  on the surface of  $\text{ZrO}_2$ , but the crystallinity of the sample was decreased by 60% compared to unsupported  $\text{ZnFe}_2\text{O}_4$  (a). A  $d$ -value was  $12 \text{ \AA}$ ,  $a = 8.233 \text{ \AA}$ , this slight decrease in  $a$  value and increase in nanocrystallite size indicates the interaction of  $\text{ZnFe}_2\text{O}_4$  and  $\text{ZrO}_2$ . XRD of catalysts samples prepared by templated method: XRD of  $\text{ZnFe}_2\text{O}_4/\text{ZrO}_2$  (d) in Fig. 1 indicates amorphous nature of the catalyst. Crystallite size is calculated by Scherrer formula (Fig. 1, Table 1).

#### 3.1.2. BET surface area measurement

Results obtained from BET surface area measurement are tabulated in Table 1 shows the interaction of  $\text{ZnFe}_2\text{O}_4$  and  $\text{ZrO}_2$ . Nanocrystallite size increases in  $\text{ZnFe}_2\text{O}_4/\text{ZrO}_2$  (CP). Due to amorphous nature of  $\text{ZnFe}_2\text{O}_4/\text{ZrO}_2$  (T) nanocrystallite size cannot be found out. Pore size of  $\text{ZnFe}_2\text{O}_4/\text{ZrO}_2$  (CP) decreases as compared to individual  $\text{ZnFe}_2\text{O}_4$  and  $\text{ZrO}_2$  and pore size of  $\text{ZnFe}_2\text{O}_4/\text{ZrO}_2$  (T) is very high;  $30 \text{ \AA}$  due to tem-

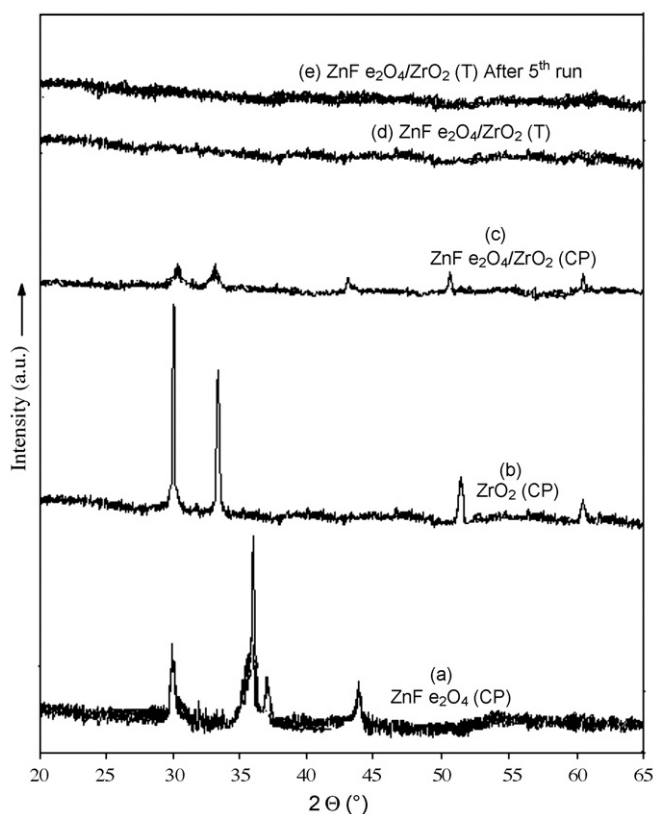


Fig. 1. X-ray diffraction pattern. (CP): co-precipitation method, (T): templated method.

templated assisted route. Similar trend is observed in surface area which is very high for  $\text{ZnFe}_2\text{O}_4/\text{ZrO}_2$  (T). From Fig. 2 the nitrogen adsorption–desorption isotherm shown in Fig. 2 is a type-IV isotherm, as defined by the IUPAC, with a sharp step at intermediate relative pressures with an H2 hysteresis loop due to capillary condensation. The isotherm, shows three well-defined stages can be identified: (a) a slow increase in nitrogen uptake at 0.0–0.15 relative pressures, corresponding to monolayer–multilayer adsorption on the pore walls, (b) a sharp step at 0.15–0.70 relative pressures indicative of capillary condensation in mesopores and (c) a plateau at 0.70–0.95 relative pressures associated with multilayer adsorption on the external surface. As observed from pore size distribution, a major part of the surface area is contributed by pores with a diameter characteristic of pores ranging from 20 to 37 Å, as shown the pore size distribution (Fig. 3) the catalyst is mesoporous in nature.

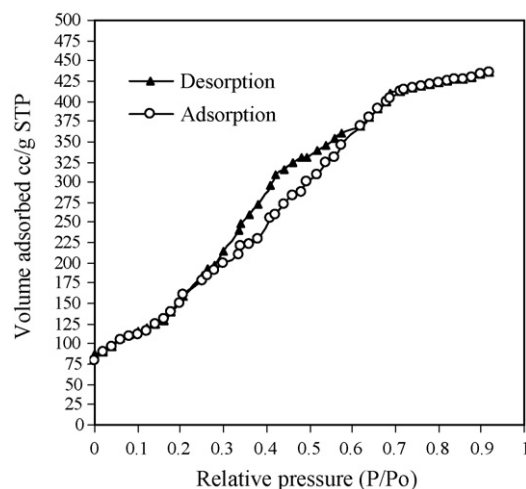


Fig. 2. Hysteresis of  $\text{N}_2$  adsorption/desorption over the surface of  $\text{ZnFe}_2\text{O}_4/\text{ZrO}_2$  (T).

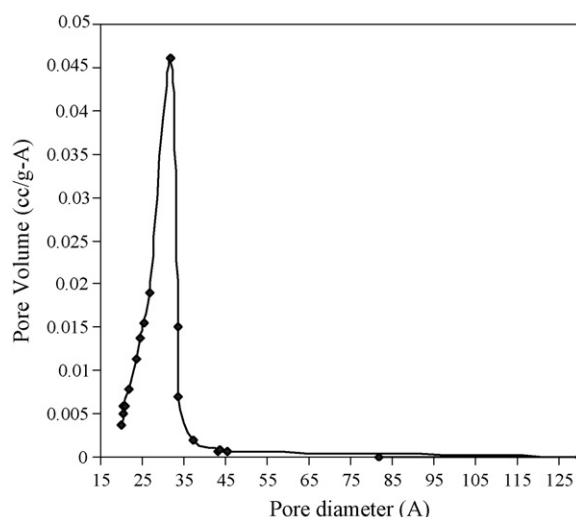


Fig. 3. Pore size by  $\text{N}_2$  adsorption/desorption of  $\text{ZnFe}_2\text{O}_4/\text{ZrO}_2$  (T).

Table 1  
Characterization of catalysts

Oxide	Precursor	Nanocrystallite size <sup>a</sup> (Å)	Pore size <sup>b</sup> (Å)	BET surface area (m <sup>2</sup> /g)	Physical properties
$\text{ZnFe}_2\text{O}_4$ (CP)	$\text{Zn}(\text{NO}_3)_2$ and $\text{Fe}(\text{NO}_3)_3$	10	3.8	17	Semiconductor
$\text{ZrO}_2$ (CP)	$\text{ZrOCl}$	8	6.2	24	Dielectric
$\text{ZnFe}_2\text{O}_4/\text{ZrO}_2$ (CP)	$\text{Zn}(\text{NO}_3)_2$ , $\text{Fe}(\text{NO}_3)_3$ and $\text{ZrOCl}$	12	4.7	20	Semiconductor
$\text{ZnFe}_2\text{O}_4/\text{ZrO}_2$ (T)	$\text{Zn}(\text{NO}_3)_2$ , $\text{Fe}(\text{NO}_3)_3$ and $\text{ZrOCl}$	–	30	180	Semiconductor

<sup>a</sup> Scherrer equation.

<sup>b</sup> BET measurement.

### 3.1.3. FT-IR measurement

Pyridine adsorbed FT-IR of  $\text{ZnFe}_2\text{O}_4/\text{ZrO}_2$  (T) the bands observed at  $\sim 1635$ ,  $\sim 1493$  and  $\sim 1541$   $\text{cm}^{-1}$  are assigned to pyridine molecules bound to Brönsted acid sites and shows peaks at  $\sim 1612$ ,  $\sim 1490$ , and  $\sim 1448$   $\text{cm}^{-1}$  that are due to pyridine molecules bound to Lewis acid sites (Fig. 4).

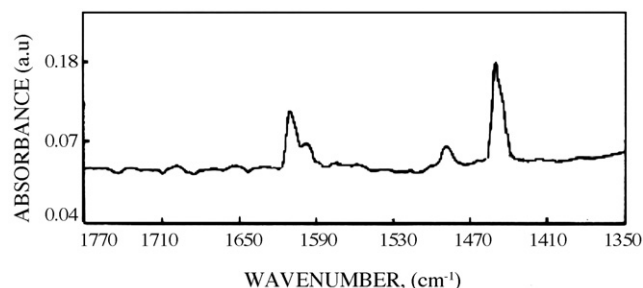


Fig. 4. Pyridine adsorbed FT-IR of  $\text{ZnFe}_2\text{O}_4/\text{ZrO}_2$  (T).

### 3.1.4. SEM measurement

SEM of  $\text{ZnFe}_2\text{O}_4/\text{ZrO}_2$  (CP) shows the aggregates of crystallites which indicate that due aggregation of the catalyst particles active sites are less accessible for the reaction to occur on the surface of the  $\text{ZnFe}_2\text{O}_4/\text{ZrO}_2$  (CP). Whereas SEM of  $\text{ZnFe}_2\text{O}_4/\text{ZrO}_2$  (T) shows the rod like morphology of the catalyst particles indicating the increase in the surface area of the catalyst with more access to the active sites for the formation of glycosidic linkage, hence more and more product is favored on  $\text{ZnFe}_2\text{O}_4/\text{ZrO}_2$  (T) compared to  $\text{ZnFe}_2\text{O}_4/\text{ZrO}_2$  (CP) (Fig. 5a and b).

It was thought desirable to study various reaction parameters under otherwise similar experimental conditions to establish the reaction mechanism.

### 3.2. Choice of catalysts for glycosylation reaction

To check effect of various catalysts for glycosidic bond formation, reaction between fatty alcohol and D-glucose were taken as model reaction.  $\text{CuFe}_2\text{O}_4$ ,  $\text{ZnFe}_2\text{O}_4$ ,  $\text{CoFe}_2\text{O}_4$ ,  $\text{NiFe}_2\text{O}_4$  and 10% (w/w)  $\text{ZnFe}_2\text{O}_4$  supported on  $\text{SiO}_2$  and  $\text{ZrO}_2$  were used to assess their efficacy in glycosylation reaction (see Table 2). As per the trend Cu containing spinels show low room temperature resistivity compared to Zn containing spinels that can be explained on the basis of a valency exchanged mechanism [14]. It is believed that, greater the energy of activation, greater will

Table 2  
Effect of various catalysts prepared by co-precipitation method

Catalyst	Room temperature resistivity	Time (h)	% conversion to APG
$\text{CuFe}_2\text{O}_4$	0.19	6	50
$\text{NiFe}_2\text{O}_4$	0.37	10	55
$\text{CoFe}_2\text{O}_4$	0.27	11	52.5
$\text{ZnFe}_2\text{O}_4$	0.59	4	60

[Catalyst]: 0.0088 g/cm<sup>3</sup>; D-glucose: 10 mM; *n*-meristyl alcohol: 20 mM; speed of agitation: 900 rpm; temperature: 363 K.

be the energy required for electronic transition resulting in the decrease in the activity of the catalyst. Hence, from energy of activation values  $\text{CuFe}_2\text{O}_4$  (0.19),  $\text{ZnFe}_2\text{O}_4$  (0.59),  $\text{CoFe}_2\text{O}_4$  (0.27) and  $\text{NiFe}_2\text{O}_4$  (0.37),  $\text{CuFe}_2\text{O}_4$  should exhibit highest and  $\text{ZnFe}_2\text{O}_4$  lowest catalytic activity at the reaction temperature. To our surprise the trend is exactly reversed.  $\text{ZnFe}_2\text{O}_4$  showed the highest conversion towards glycosidic bond formation to give alkyl poly- $\beta$ -D-glucopyranoside. The most probable reasons to these observations are: (1) In  $\text{ZnFe}_2\text{O}_4$ , tetrahedral site is occupied by  $\text{Zn}^{2+}$  ions and octahedral site is occupied by  $\text{Fe}^{3+}$ . In  $\text{Zn}^{2+}$ ,  $d^{10}$  orbitals are more contracted than any other transition metal ion d-orbital. The decreased overlap of the oxygen 2p, 3d and 4s with the  $\text{Fe}^{3+}$  at octahedral site has an indirect but appreciable effect on the hopping process. Catalytic activity is mainly due to the hopping of  $\text{Fe}^{3+}$  from octahedral site to tetrahedral site. Thus in spinel lattice cation distribution plays an important role in the reaction. Also it is well known that p-type of semiconductors is active and selective towards dehydrogenation owing to rapid migration of holes. From thermoelectric power measurements it can be concluded that in  $\text{CuFe}_2\text{O}_4$  concentration of holes is less hence dehydrogenation selectivity decreases from  $\text{ZnFe}_2\text{O}_4$  to  $\text{CuFe}_2\text{O}_4$  so the selective formation of the product is more. (2) In  $\text{ZnFe}_2\text{O}_4$  as  $\text{Zn}^{2+}$  and  $\text{O}^{2-}$  overlap is poor, Zn–O bond is weak hence lattice oxygen can be easily exchanged with the substrate molecule, resulting in the increasing dehydrogenation activity.

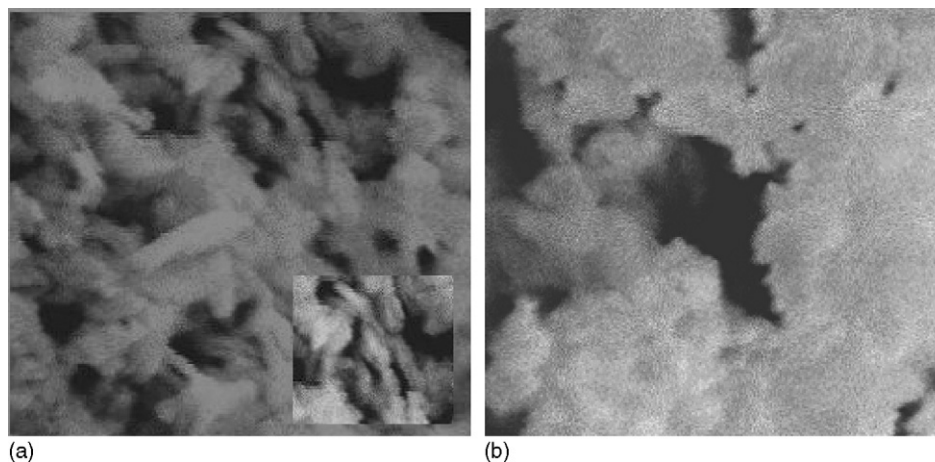


Fig. 5. (a) SEM of  $\text{ZnFe}_2\text{O}_4/\text{ZrO}_2$  (CP) and (b) of  $\text{ZnFe}_2\text{O}_4/\text{ZrO}_2$  (T).

Table 3  
(1) and (2) Effect of support and preparation procedure

1		2	
Catalyst/support	% conversion to APG	Preparation procedure of ZnFe <sub>2</sub> O <sub>4</sub> /ZrO <sub>2</sub>	% conversion to APG
ZnFe <sub>2</sub> O <sub>4</sub> /SiO <sub>2</sub>	66.0	Co-precipitation (CP)	70.0
ZnFe <sub>2</sub> O <sub>4</sub> /ZrO <sub>2</sub>	70.0	Templated route (T)	83.0

[Catalyst]: 0.0088 g/cm<sup>3</sup>; D-glucose: 10 mM; *n*-meristyl alcohol: 20 mM; speed of agitation: 900 rpm; temperature: 363 K.

### 3.3. Effect of support (catalysts are prepared by co-precipitation)

To study the effect of support 10% (w/w) ZnFe<sub>2</sub>O<sub>4</sub> was supported on SiO<sub>2</sub> and ZrO<sub>2</sub>. ZnFe<sub>2</sub>O<sub>4</sub>/ZrO<sub>2</sub> was found to be the best catalyst with 70% conversion of *n*-decanol leading to the formation of alkyl poly-β-D-glucopyranoside. This may be due to increased in surface area and nature of the support. ZrO<sub>2</sub> is amphoteric in nature whereas SiO<sub>2</sub> is acidic. It was observed that when ZnFe<sub>2</sub>O<sub>4</sub>/SiO<sub>2</sub> were used formation of alkyl poly-β-D-glucopyranoside was suppressed and polyglucose that is; glucose–glucose condensation was favoured product. When ZnFe<sub>2</sub>O<sub>4</sub>/ZrO<sub>2</sub> were used formation of alkyl poly-β-D-glucopyranoside was the main product and polyglucose formation was suppressed. Thus acidity of ZnFe<sub>2</sub>O<sub>4</sub> was tuned by supporting it with ZrO<sub>2</sub> for further study 10% (w/w) ZnFe<sub>2</sub>O<sub>4</sub>/ZrO<sub>2</sub> was used (Table 3 (1)).

### 3.4. Effect of preparation procedure

A 10% (w/w) ZnFe<sub>2</sub>O<sub>4</sub>/ZrO<sub>2</sub> was prepared by two different methods, viz, co-precipitation and templated approach. It was seen that catalyst prepared by templated approach showed 83% formation of alkyl poly-β-D-glucopyranoside (Table 3 (2)). Increase in the surface area and pore size leads to increase in more product formation. In co-precipitation method hydrolysis of the salts takes place very fast so there is no chance for the catalyst to increase the surface area, while in templated approach hydrolysis of the metal salt takes place very slowly in controlled manner due to presence of the template, decly poly-glucoside. The formation of metal template complex followed by hydrolysis leads to the formation of mesopores in the catalyst which is retained after calcinations. Hence increases the surface area leading to increasing product formation.

### 3.5. Effect of solvent

Variety of solvents was used for the reaction as shown in Fig. 6. It was seen that in case of acetic acid due to its acidic nature degree of polymerization of glucose was more and the colour of the product also suffered which is undesirable. We have also checked the reaction without catalyst in acetic acid, in this case we failed to obtain alkyl poly-β-D-glucopyranoside, and instead we obtained only poly glucose. Thus it was confirmed that catalysts plays the major role in the formation of alkyl poly β-D-glucopyranoside. When dimethyl sulfoxide,

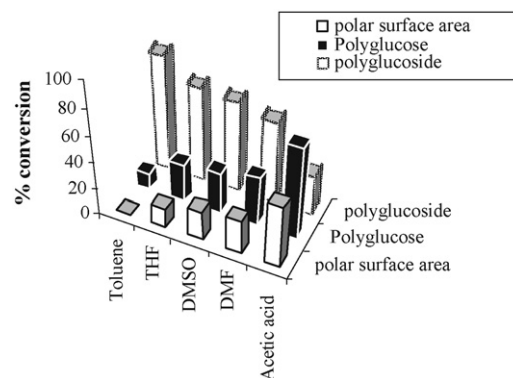


Fig. 6. Effect of solvents. Catalyst: ZnFe<sub>2</sub>O<sub>4</sub>/ZrO<sub>2</sub> (T); [Catalyst]: 0.0088 g/cm<sup>3</sup>; D-glucose: 10 mM; *n*-meristyl alcohol: 20 mM; speed of agitation: 900 rpm; temperature: 363 K.

dimethylformamide and tetrahydrofuran were used as solvent, though degree of polymerization was in range but separation of the major product from the reaction mass and solvent recovery was difficult. In dimethyl sulfoxide the product obtained had undesirable odor. Polar surface area of solvents increase from toluene < THF < DMSO < DMF < acetic acid, this increase in polar surface area, increases the formation of polyglucose suppressing the formation of alkyl poly-β-D-glucopyranoside. Hence the formation of alkyl poly-β-D-glucopyranoside was more in toluene and product obtained was yellowish with degree of polymerization in desirable range, also the solvent recovery was easy. All further reactions were taken in toluene as reaction media.

### 3.6. Effect of temperature

The effect of temperature on conversion under otherwise similar conditions was studied in the range of 323–373 K as shown in the Fig. 7. It was seen that the initial conversion increased up to 363 K and there after decreased due to charring of glucose with increasing temperature. At 373 K alkyl poly-β-D-glucopyranoside was also charred which gave dark color and

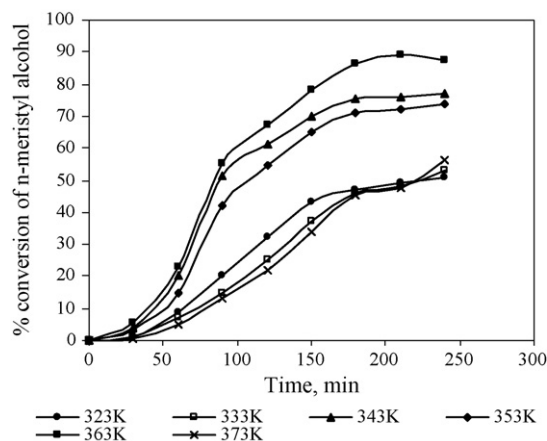


Fig. 7. Effect of temperature. Catalyst: ZnFe<sub>2</sub>O<sub>4</sub>/ZrO<sub>2</sub> (T); [Catalyst]: 0.0088 g/cm<sup>3</sup>; D-glucose: 10 mM; *n*-meristyl alcohol: 20 mM; speed of agitation: 900 rpm; solvent: toluene.

Table 4  
Product analysis

Alcohol chain length	Conversion to APG (%)	MP (°C)	$[\alpha]_D^{25}$	$^1\text{H}$ NMR data of $\beta$ -D-glycoside	IR KBr ( $\text{cm}^{-1}$ )	Elemental analysis					
						Calculated			Observed		
						C	H	O	C	H	O
<i>n</i> -Octanol	75.0	62.0	33.8	4.09 (d, $J=7.8$ Hz)	3412, 2928, 2831, 1075, 1030	57.53	9.58	32.89	57.50	9.60	32.90
<i>n</i> -Decanol	78.0	135.6	27.8	4.09 (d, $J=7.8$ Hz)	3386, 2925, 2829, 1080, 1036	60.75	10.12	29.13	60.78	10.15	29.07
<i>n</i> -Dodecanol	80.0	144.5	22.7	4.09 (d, $J=7.8$ Hz)	3390, 2935, 2821, 1085, 1040	65.85	10.36	23.79	65.83	10.35	23.82
<i>n</i> -Meristyl alcohol	87.2	–	–	4.09 (d, $J=7.8$ Hz)	3412, 2928, 2831, 1075, 1030	70.58	13.52	15.94	70.57	13.50	15.93

Catalyst:  $\text{ZnFe}_2\text{O}_4/\text{ZrO}_2$  (T); [Catalyst]:  $0.0088 \text{ g/cm}^3$ ; D-glucose: 10 mM; fatty alcohol: 20 mM; speed of agitation: 900 rpm; temperature: 363 K.

odor to the final product. While at 363 K said problems was not encountered so further studies were done at 363 K.

### 3.7. Effect of alcohols

To investigate the effect of chain length of fatty alcohols, glycosylation was also carried out with  $\text{C}_8$ ,  $\text{C}_{10}$ ,  $\text{C}_{12}$  and  $\text{C}_{14}$  under otherwise similar conditions. Table 4 summarizes the optimized results of alkyl poly- $\beta$ -D-glucopyranosides of several alcohols over  $\text{ZnFe}_2\text{O}_4/\text{ZrO}_2$  (T) catalyst. It was found that the increase in the carbon chain length increases the rate of alkyl poly- $\beta$ -glycosylation reaction. The possible reason may be the faster generation of alkoxide due to increase in carbon number. All further reaction parameters were optimized using *n*-meristyl alcohol ( $\text{C}_{14}$ ).

### 3.8. Effect of speed of agitation

The effect of speed of agitation was studied in the range of 600–1500 rpm and is shown in the Fig. 8. It was found that there was practically no change in the conversion. This shows that the influence of external resistance to the transfer of substrates to the catalyst surface was absent, therefore further experiment were conducted at 900 rpm.

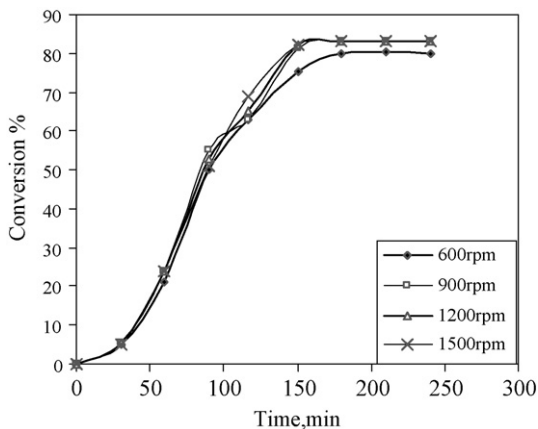


Fig. 8. Effect of speed of agitation. Catalyst:  $\text{ZnFe}_2\text{O}_4/\text{ZrO}_2$  (T); [Catalyst]:  $0.0088 \text{ g/cm}^3$ ; D-glucose: 10 mM; *n*-meristyl alcohol: 20 mM. temperature: 363 K; solvent: toluene.

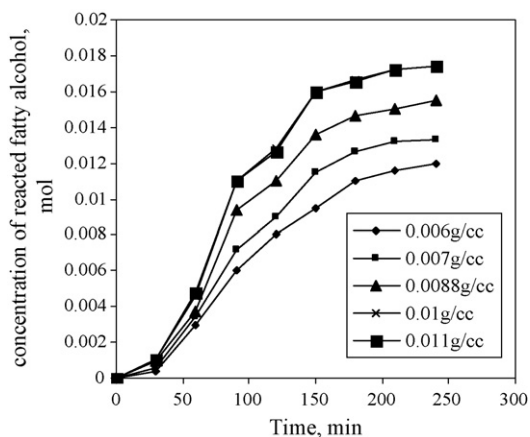


Fig. 9. Effect of catalyst concentration. Catalyst:  $\text{ZnFe}_2\text{O}_4/\text{ZrO}_2$  (T); speed of agitation: 900 rpm; D-glucose: 10 mM; *n*-meristyl alcohol: 20 mM; temperature: 363 K; solvent: toluene.

### 3.9. Effect of catalyst concentration

Rate of reaction is directly proportional to concentration of catalyst based on the entire liquid phase volume. The catalyst concentration was varied from 0.006 to  $0.011 \text{ g/cm}^3$  on the basis of total volume of the reaction mixture keeping all other conditions similar. Fig. 9 shows the effect of concentration of catalyst on the formation of alkyl poly- $\beta$ -D-glucopyranoside. The con-

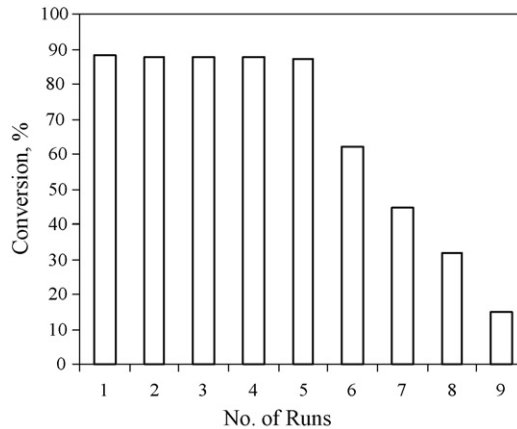
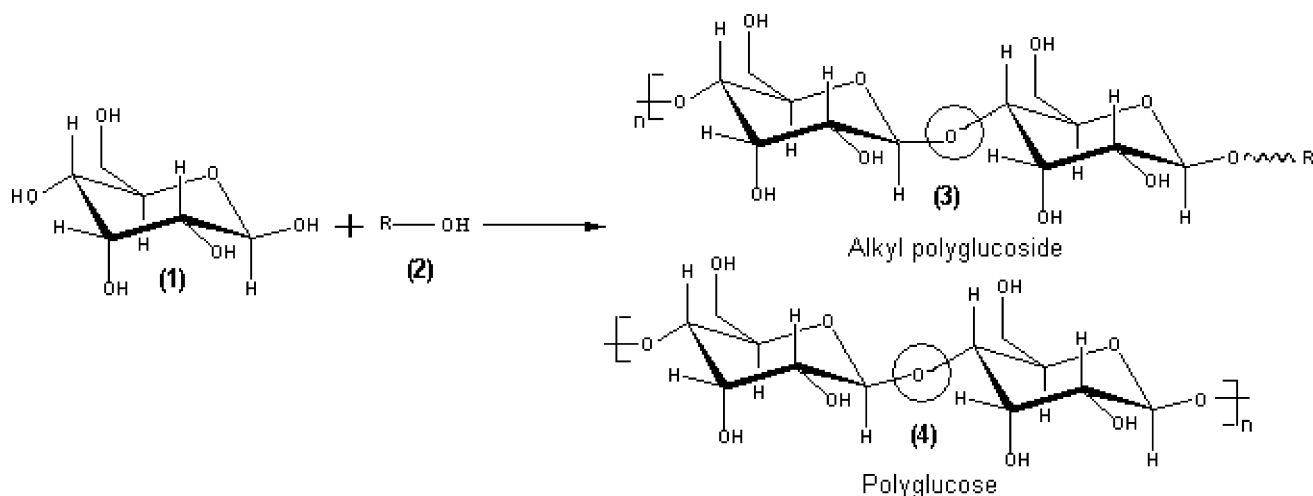


Fig. 10. Catalyst reusability and stability. Catalyst:  $\text{ZnFe}_2\text{O}_4/\text{ZrO}_2$  (T); [Catalyst]:  $0.0088 \text{ g/cm}^3$ ; speed of agitation: 900 rpm; D-glucose: 10 mM; *n*-meristyl alcohol: 20 mM; temperature: 363 K; solvent: toluene.



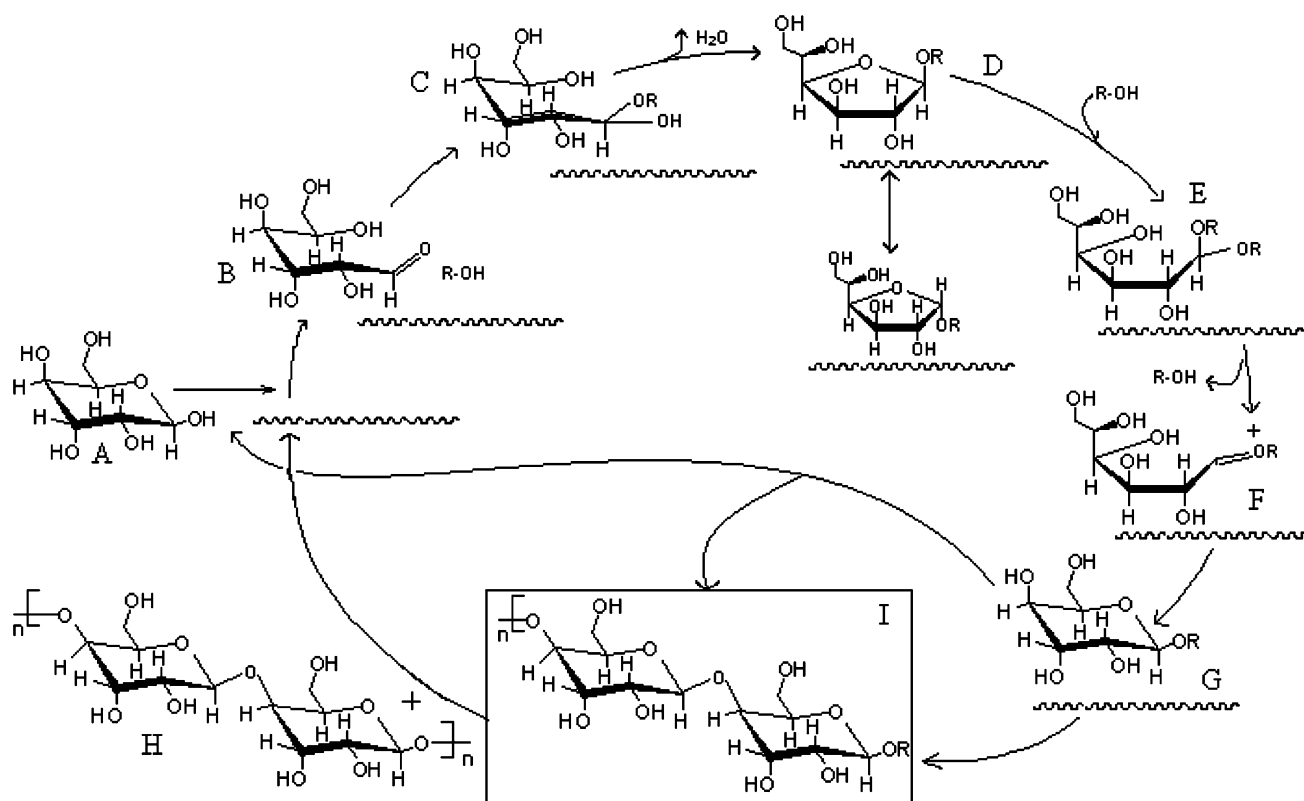
Scheme 1. Reaction of glucose and fatty alcohol.

version increased with increase in concentration of catalyst, which is due to the proportional increase in the number of active sites. However, beyond 0.0088 g/cm<sup>3</sup> concentration of catalyst, there was no significant increase in the conversion and hence all further experiments were carried out at this catalyst loading.

### 3.10. Catalyst reusability and stability

ZnFe<sub>2</sub>O<sub>4</sub>/ZrO<sub>2</sub> (T) catalyst has good reusability and without pretreatment it can show selective conversion up to

five cycles (see Fig. 10). The catalyst was easily recovered by filtration and could be reused five times for the alkyl poly-β-glycosylation reaction without affecting the activity or selectivity of the process. After fifth run the activity of the catalyst decreases, the XRD pattern of the used catalyst shows no structural deterioration. The decrease in activity can be attributed to pore blockage by deposition due to which active sites become inaccessible. The catalysts can be easily reactivated after washing it with acetone and treating it at 373 K for 24 h.

Scheme 2. Reaction of glucose and fatty alcohol over the surface of the ZnFe<sub>2</sub>O<sub>4</sub>/ZrO<sub>2</sub> (T) catalyst to afford poly-β-D-alkyl glucopyranoside and poly-glucopyranoside.

#### 4. Reaction and reaction mechanism

The  $\beta$ -glycosidic bond formation of D-glucose with alcohol is one-step reaction as shown in Scheme 1 (see glycosidic bond formation in the circle, R = C<sub>8</sub>–C<sub>14</sub> alcohols). In the above reaction (3) is the major product whereas (4) is side product. Formation of (4) alters the physico-chemical property of polyglycosides so product (4) is undesirable, hence reaction suffers and application of the product is restricted.

The most satisfactory mechanism for Fischer glycosylation was proposed by Levene et al. [15], in which aldoses or ketones on treatment with alcohols containing acid catalysts yield glycosides as a major product. The major reaction takes place usually via  $\alpha$ -furanoside or  $\beta$ -furanoside formation. Such intermediates further convert to pyranosides. For present catalytic system we suggest following mechanism. D-Glucose (A) shows anomericization of pyranose form which presumably is occurring rapidly under acidic conditions [16]. This anomericization occurs through ring opening followed by addition of fatty alcohol (B) to form unstable intermediate (C) and loss of water molecule to form  $\alpha$ -furanoside or  $\beta$ -furanoside (D). Presently we are not sure about the exact anomeric form of furanoside; however the major product is alkyl poly- $\beta$ -D-glucopyranoside. Another alcohol molecule addition and elimination in furanose (D) gives alkyl poly- $\beta$ -D-glucopyranoside as a major product as shown in (G). The formation of alkyl poly- $\beta$ -D-glucopyranoside occurs due to attack of –OH of C<sub>1</sub> of D-glucose (A) on –OH of C<sub>4</sub> of alkyl  $\beta$ -D-glucopyranoside (G). The alkyl poly- $\beta$ -D-glucopyranoside shows inside the rectangular box (Scheme 2).

During the course of the reaction, as the catalyst surface is acidic, formation of polyglucose (H) takes place. Polyglucose formation occurs due to attack of –OH of C<sub>1</sub> of D-glucose (A) on –OH of C<sub>4</sub> of another D-glucose (A). After the formation of the product on the surface of the catalyst, desorption of the product takes place and the surface of the catalyst again starts the new reaction cycle with the adsorption of glucose and fatty alcohol.

#### 5. Conclusion

The efficacy of different catalysts was evaluated at 363 K with 0.0088 g/cm<sup>3</sup> catalyst loading and toluene as a reaction solvent at 900 rpm. ZnFe<sub>2</sub>O<sub>4</sub>/ZrO<sub>2</sub> (T) prepared by template route shows excellent conversion and selectivity towards alkyl poly- $\beta$ -D-glucopyranosides due to increase in surface area of the catalyst. C<sub>14</sub> fatty alcohol shows maximum formation of alkyl poly- $\beta$ -D-glucopyranosides because of the ease of alkoxide formation. The catalyst could be reused five times and was easily recovered by filtration without affecting the activity or selectivity of the process.

#### References

- [1] H. Wong, G. Whitesides, *Enzymes in Synthetic Organic Chemistry*, 12, Pergamon Press, Oxford, 1994, pp. 252–311.
- [2] K. Faber, *Biotransformation in Organic Chemistry: A Text Book*, 4th ed., Springer-Verlag, Berlin, 2000, p. 307.
- [3] T. Boecker, *J. Tenside Surf. Deter.* 26 (1989) 318.
- [4] J. Banoub, D. Bundle, *Can. J. Chem.* 57 (1979) 2085.
- [5] H. Paulsen, M. Paal, *Can. J. Chem.* 135 (1984) 53.
- [6] K. Jansson, S. Ahlfors, T. Frejd, J. Kihlberg, G. Magnusson, J. Dahmen, G. Noori, K. Stenvall, *J. Org. Chem.* 53 (1988) 5629.
- [7] T. Jyojima, N. Miyamoto, Y. Ogawa, S. Matsumara, K. Toshima, *Tet. Lett.* 40 (1999) 5023–5026.
- [8] H. Nagai, S. Matsumura, K. Toshima, *Tet. Lett.* 43 (2002) 847–850.
- [9] V. Joshi, M. Sawant, *Ind. J. Chem.* 45B (2006) 461–465.
- [10] N. Chaubal, M. Sawant, *Ind. J. Chem.* 43A (2004) 1427.
- [11] V. Parmar, B. Modi, H. Kunal, H. Joshi, *Ind. J. Pure Appl. Phys.* 37 (3) (1999) 207.
- [12] B. Mulla, V. Darshane, *Ind. J. Chem.* 22A (1983) 143.
- [13] N. Chaubal, M. Sawant, *J. Mol. Catal. A: Chem.* 261 (2006) 232–241.
- [14] J. Vervev, P. Brown, F. Groter, F. Romeijn, V. Santhu, *Phys. Chem.* 5 (1951) 198.
- [15] (a) P. Levene, A. Raymond, R. Dillon, *J. Biol. Chem.* 95 (1932) 699; (b) V. Smirnyagin, C. Bishop, *Can. J. Chem.* 46 (1968) 3085.
- [16] B. Capron, *Chem. Rev.* 69 (4) (1969) 407–498.